Supplementary Figures

Supplementary Figure 1. (column width)

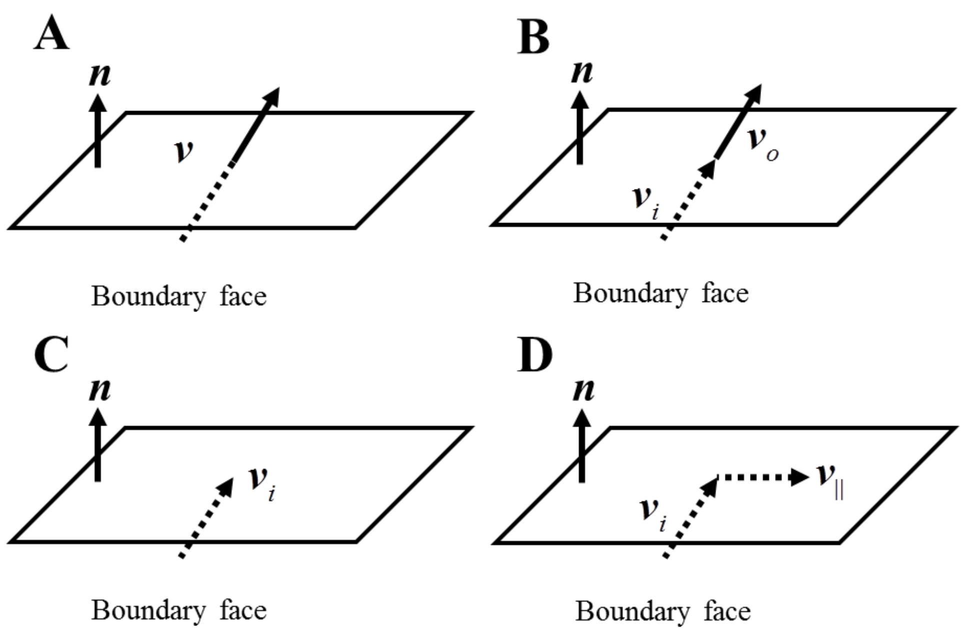

Supplementary Figure 1. Vessel boundary conditions in the growth model. Vectors inside the mesh are dashed, vectors outside are solid. (A) When a segment was found to grow outside the mesh and through a boundary face, the segment was split into an inside component, $\boldsymbol{v}_i$, and an outside component, $\boldsymbol{v}_o$ (B). There were two different types of boundary conditions enforced on microvessels during growth. (C) Mesh boundary: The faces of the mesh at the symmetry planes and any fully constrained face representing the stainless steel mesh were considered mesh boundaries. When a vessel encountered one of these boundaries, the outside component was disregarded and growth ended at the point where the segment intersected the boundary face. (D) Gel boundary: Unconstrained faces of the mesh were considered gel boundaries and represent the external surface of the gel that contacts the growth media. When a vessel encountered this type of boundary, its outside component was projected into the plane of the boundary face. The outside component was replaced with this projection, $\boldsymbol{v}_{\|}$, causing the vessel to change direction and start growing within the plane of the boundary.

Supplementary Figure 2. (column width)

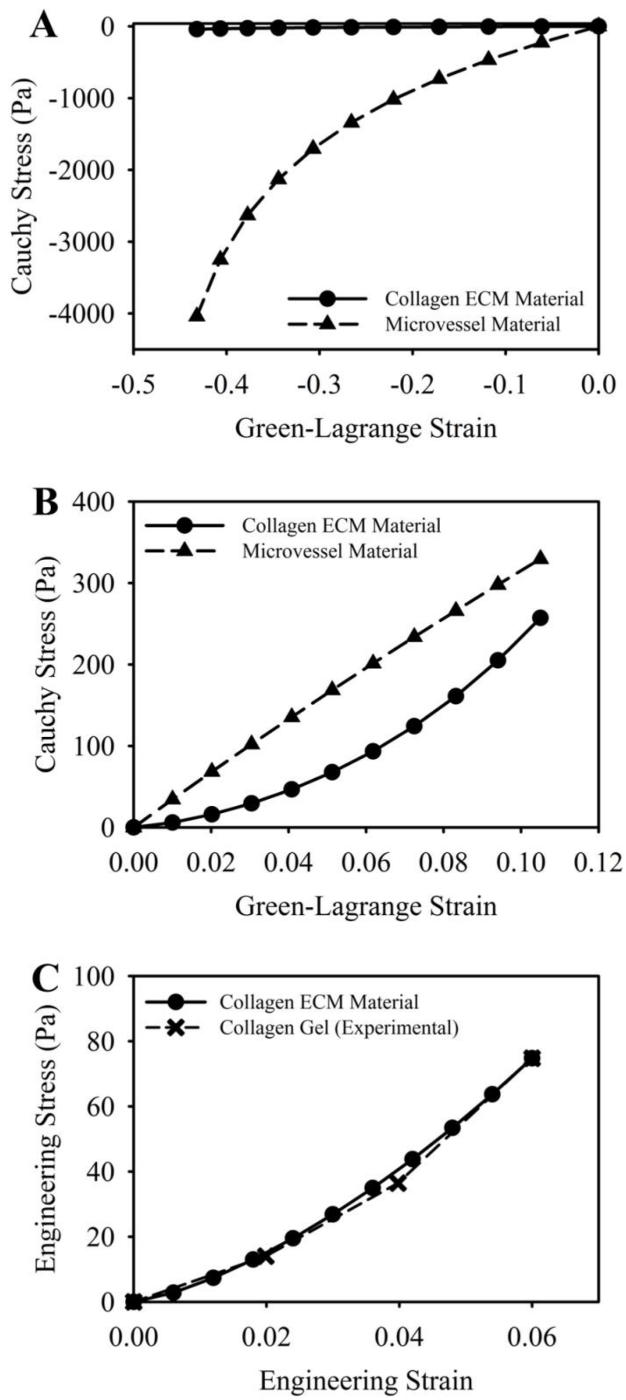

Supplementary Figure 2. Stress-strain plots for the material model used in the simulation. A composite material was used to account for the properties of both the acellular ECM and the microvessel network. This material uses a weighted average of the ECM and microvessel stress response to determine the stress for the composite as a whole. (A) Cauchy stress vs. Green-Lagrange strain for the ECM and microvessel materials in compression. Minimum principal strain within the simulations reached -0.4. The ECM material offers very little stress to resist compression compared to the microvessel material. (B) Cauchy stress vs. Green-Lagrange strain for the ECM and microvessel materials in tension. Maximum principal strain within the simulations reached 0.1. The ECM material acts much stiffer in tension than in compression, demonstrating the tension-compression non-linear for this material. (C) Engineering stress vs. engineering strain for the ECM material. Data from uniaxial extension of 3.0 mg/ml collagen gels was used to set the modulus of the ECM material in tension, E_{fib}. Experimental data is presented as the dashed line with 'x' markers, while the material fit is presented as the solid line with circular markers. Our material model was able to produce excellent agreement with the experimental data within the range of data tested during the experiment.